Radiotherapy and Oncology xxx (2015) xxx–xxx

Contents lists available at ScienceDirect

Radiotherapy and Oncology

journal homepage: www.thegreenjournal.com

Original article

Short-term pretreatment DCE-MRI in prediction of outcome in locally advanced cervical cancer

Kjersti V. Lund [a,b], Trude G. Simonsen [a], Tord Hompland [a], Gunnar B. Kristensen [c,d,e], Einar K. Rofstad [a,*]

[a] Department of Radiation Biology, Institute for Cancer Research; [b] Department of Radiology and Nuclear Medicine; [c] Department of Gynecological Cancer; [d] Institute for Cancer Genetics and Informatics, Oslo University Hospital; and [e] Institute for Clinical Medicine, University of Oslo, Norway

ARTICLE INFO

Article history:
Received 5 December 2014
Received in revised form 17 March 2015
Accepted 1 May 2015
Available online xxxx

Keywords:
Cervical carcinoma
Concurrent chemoradiotherapy
DCE-MRI
Semiquantitative analysis
Treatment outcome

ABSTRACT

Background and purpose: Several investigators have indicated that dynamic contrast-enhanced magnetic resonance imaging (DCE-MRI) has the potential to provide biomarkers for personalized treatment of cervical carcinoma. However, some clinical studies have suggested that treatment failure is associated with low tumor signal enhancement, whereas others have reported associations between high signal enhancement and poor outcome. The purpose of this investigation was to clear up these conflicting reports and to provide a method for identifying biomarkers that easily can be implemented in routine DCE-MRI diagnostics.

Methods: The study involved 85 patients (FIGO stage IB through IVA) treated with concurrent chemoradiotherapy. Low-enhancing tumor volume (LETV) and low-enhancing tumor fraction (LETF), defined as the volume and fractional volume of low-enhancing voxels, respectively, were calculated from signal intensities recorded within 1 min after contrast administration by using two methods reported to give conflicting conclusions.

Results: Multivariate analysis involving tumor volume, lymph node status, FIGO stage, and LETV or LETF revealed that LETV and LETF provided independent prognostic information on treatment outcome, independent of the method of calculation.

Conclusion: Low signal enhancement is associated with poor prognosis in cervical carcinoma, and biomarkers predicting poor outcome can be provided by short-term DCE-MRI without advanced image analysis.

The recommended treatment of locally advanced carcinoma of the uterine cervix is cisplatin-based concurrent chemoradiotherapy [1]. The rate of recurrence is significant and the incidence of severe complications is high, and therefore, it has been suggested that the outcome may be improved by personalizing the treatment [1–3]. Because treatment failure and poor survival rates are strongly associated with extensive hypoxia in the primary tumor in patients treated with radiation therapy [4–10], personalized treatment strategies require novel biomarkers reflecting the oxygenation status of the tumor tissue [2,3].

Accumulated evidence from preclinical and clinical studies suggests that dynamic contrast-enhanced magnetic resonance imaging (DCE-MRI) with gadolinium diethylene-triamine penta-acetic acid (Gd-DTPA) as contrast agent has the potential to provide information on the oxygenation of cervical carcinomas [11–18]. Moreover, initial investigations of the prognostic power of DCE-MRI have revealed that DCE-MRI-derived data may be associated with local tumor control, disease-free survival, and overall survival in patients with advanced disease [19–25].

However, apparently conflicting observations have been reported. Treatment failure and poor survival were associated with high signal enhancement in some studies [25,26] and with low signal enhancement in others [27,28]. For example, Donaldson et al. [26] measured the fraction of voxels that showed significant signal enhancement (i.e., a signal enhancement greater than three times the standard deviation of the pre-contrast signals) and found that high enhancing fraction (EF) at 25 s post-contrast was associated with poor disease-free survival. In contrast, Mayr et al. [27] generated histograms of the relative signal intensity (i.e., the ratio of post- to pre-contrast signal intensity) at ~60 s post contrast, determined the number of voxels with relative signal intensity <2.1, and showed that a high value of this signal intensity (SI) parameter was associated with low rates of local tumor control and disease-specific survival.

In the investigation reported here, pretreatment DCE-MRI data of a cohort of 85 patients with locally advanced carcinoma of the

* Corresponding author at: Department of Radiation Biology, Institute for Cancer Research, Norwegian Radium Hospital, Box 4953 Nydalen, 0424 Oslo, Norway.
E-mail address: einar.k.rofstad@rr-research.no (E.K. Rofstad).

http://dx.doi.org/10.1016/j.radonc.2015.05.001
0167-8140/

uterine cervix were analyzed by using both the EF-method of Donaldson et al. [26] and the SI-method of Mayr et al. [27]. We demonstrate that these methods provide almost identical numbers of low-enhancing voxels and show that poor disease-free and overall survival rates are associated with low signal enhancement, in accordance with the study of Mayr et al. [27] but in contrast to that of Donaldson et al. [26].

Materials and methods

Patients

A cohort of 85 consecutive patients recruited to the chemoradiotherapy protocol for previously untreated locally advanced cervical cancer (FIGO stage IB through IVA) at the Norwegian Radium Hospital between September 2004 and May 2007 was included in the study. This cohort includes the patients that were examined with respect to the predictive power of peritumoral interstitial fluid flow velocity in a previous study [29]. The characteristics of the patients are summarized in Supplementary Table 1.

The patients were treated with concurrent chemoradiotherapy with curative intent. External beam radiation therapy was given in 25 fractions during a period of 5 weeks to a total dose of 50 Gy to the primary tumor, parametria, and adjacent pelvic wall and 45 Gy to the rest of the pelvic region. In addition, 5–6 fractions of intracavitary brachytherapy with a dose of 4.2 Gy per fraction were given to Point A. Chemotherapy with cisplatin (40 mg/m^2) was given weekly with a maximum of 6 courses during the radiation therapy period.

The patients were followed up by clinical examinations every third month for the first 2 years and thereafter every sixth month. The primary endpoints were disease-free survival (DFS), defined as the time to local or distant relapse or death from any cause measured from the date of diagnosis, and overall survival (OS), defined as the interval from diagnosis to death from any cause. DFS and OS curves were generated by using the Kaplan–Meier method. Median follow-up was 5.5 years (range 1.7–7.3 years).

The investigations were approved by the regional committee of medical research ethics in southern Norway and were conducted in accordance with the Declaration of Helsinki. Written informed consent was obtained from each patient.

Magnetic resonance imaging

A 1.5-T whole-body scanner (Signa; General Electric) and a 4-channel phased-array surface coil were used for MRI. The entire pelvic region was scanned with an axial T_2-weighted fast spin echo sequence (TR = 4960 ms, TE = 84 ms, field of view: 20×20 cm^2, image matrix: 512×512, number of excitations: 1.5, slice thickness: 5 mm, slice spacing: 6 mm). DCE-MRI was carried out by using an axial T_1-weighted spoiled gradient recalled sequence (TR = 160 ms, TE = 3.5 ms, $\alpha_{T1} = 90°$, field of view: 20×20 cm^2, image matrix: 256×256, number of excitations: 1, slice thickness: 5 mm, slice spacing: 6 mm). Three T_1-weighted images were acquired before a bolus of 0.1 mmol/kg Gd-DTPA was administered, and T_1-weighted images were recorded at a temporal resolution of 29 s after the Gd-DTPA administration. The MRI was carried out before treatment was initiated.

Tumor volume and lymph node status

Primary tumor volume and lymph node status were determined by examining MR images in the open source dicom viewer Osirix [30]. A region of interest (ROI) encompassing the tumor area was drawn in the T_2-weighted images. Tumor volume was calculated from three orthogonal diameters using the formula of an ellipsoid. Lymph node status was determined by examining the internal, external, and lower common iliac chains. A lymph node was scored as metastasis-positive when its shortest diameter in the T_2-weighted images was longer than 1.0 cm and the T_1-weighted images showed a contrast enhancement pattern similar to that of the primary tumor. Fine-needle aspiration cytology was used to assess lymph node status if assessment from MR images alone proved difficult.

Image processing and analysis

Voxel-by-voxel analyses of MR images were carried out by using in-house-made software developed in Matlab. Minor tumor movements during the DCE-MRI were corrected for by coordinate mapping. Relative signal intensity was calculated as the ratio of post- to pre-contrast signal intensity, using the mean of the three pre-contrast voxel values and the value of the corresponding voxel in the first, second, third, and fourth post-contrast image as well as the mean value calculated from the first and second post-contrast images. To diminish any consequences of noise and to ease comparisons with the studies of Donaldson et al. [26] and Mayr et al. [27], the figures and data presented in this communication refer to the last-mentioned parameter, corresponding to 29–58 s after contrast administration.

Donaldson et al. [26] defined voxels showing a signal enhancement less than three times the standard deviation of the pre-contrast signals as low-enhancing voxels, and Mayr et al. [27] defined voxels with relative signal intensity <2.1 as low-enhancing voxels. We analyzed our data by using threshold values for standard deviation ranging from 1.5 to 16 in increments of 0.1 and threshold values for relative signal intensity ranging from 1.1 to 2.4 in increments of 0.01. Low-enhancing tumor volume (LETV) and low-enhancing tumor fraction (LETF) were used as input parameters in the analysis. LETV was defined as the volume of the voxels with signal intensity below the threshold value for standard deviation (EF-method) or the volume of the voxels with signal enhancement below the threshold value for relative signal intensity (SI-method). LETF was calculated as the ratio of the number of low-enhancing voxels to the total number of tumor voxels. Because there is no obvious way of dividing a patient cohort into two groups, we arranged the patients in decreasing order based on LETV or LETF, and divided the cohort into two groups by using all possible combinations of cut-off values for LETV or LETF (i.e., 84 cut-off values for the 85 patients) and threshold values for standard deviation or relative signal intensity. The two groups were compared by using the log-rank test. The results are presented as *P*-value images and in selected cases as Kaplan–Meier plots. Corrections for multiple comparisons were not performed due to the exploratory nature of the work, and the study should thus be considered as hypothesis-generating. Receiver operating characteristic (ROC) analysis was used to determine robust threshold values for standard deviation and relative signal intensity. Univariate and multivariate Cox regression analyses were used to identify prognostic factors for DFS and OS. *P*-values <0.05 were considered significant.

Results

The actuarial DFS and OS at 5 years were 63% and 67%, respectively. Tumor progression or recurrence was documented in 25 patients, 7 in the pelvis alone, 3 in the pelvis and para-aortic lymph nodes or distant sites, and 15 in para-aortic lymph nodes or distant sites alone. Two patients were clinically disease-free after further treatment, whereas the other 23 patients died from their recurrences (22 patients) or intercurrent disease (1 patient). In total, 10 patients died from intercurrent diseases.

Please cite this article in press as: Lund KV et al. Short-term pretreatment DCE-MRI in prediction of outcome in locally advanced cervical cancer. Radiother Oncol (2015), http://dx.doi.org/10.1016/j.radonc.2015.05.001

Tumor signal enhancement differed substantially among individual patients. This is illustrated in Supplementary Fig. 1, which shows corresponding T_2-weighted, pre-contrast T_1-weighted, and post-contrast T_1-weighted images of a patient showing high tumor signal enhancement (Supplementary Fig. 1a) and a patient showing low tumor signal enhancement (Supplementary Fig. 1b).

P-value images for LETV are presented in Fig. 1. These images show the proportion of patients classified as having low tumor signal enhancement (i.e., large LETV) in the vertical direction and the threshold value for standard deviation or relative signal intensity in the horizontal direction, and they refer to DFS (upper panel) and OS (lower panel) analyzed by the EF-method (Fig. 1a) and the SI-method (Fig. 1b). The images are similar, regardless of whether DFS or OS was used as endpoint and regardless of whether the EF- or SI-method was used for analysis. They suggest that DFS and OS differed significantly between the patients showing low tumor signal enhancement and those showing high tumor signal enhancement and that the low tumor signal enhancement group included approximately one third of the total patient cohort. Equivalent *P*-value images for LETF are shown in Supplementary Fig. 2a and b. These images are qualitatively similar to those for LETV, showing that our observations did not depend strongly on whether the analysis was based on LETV or LETF.

ROC analysis was carried out to find optimal threshold values for standard deviation and relative signal intensity. The analysis revealed that the most robust threshold values were 4.0 for

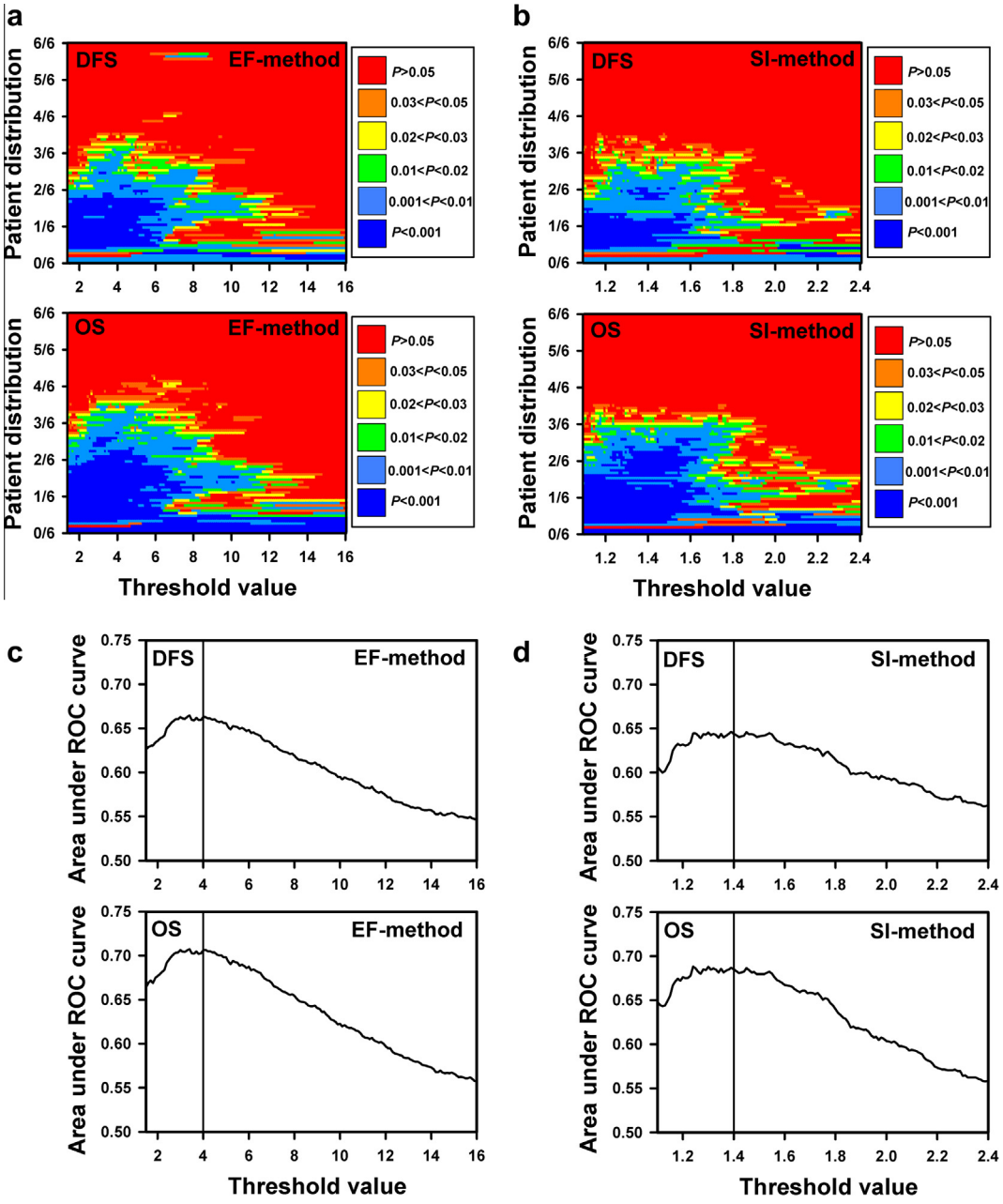

Fig. 1. *P*-value images for DFS and OS determined by the EF-method (a) and the SI-method (b) and ROC plots for DFS and OS pertaining to the EF-method (c) and the SI-method (d), based on LETV. The *P*-value images show the proportion of patients classified as having large LETVs versus the threshold value for standard deviation or relative signal intensity. Each pixel in the images represents a *P*-value given by the color code, and this *P*-value was determined by the log-rank test and refers to the combination of proportion of patients and threshold value given by the coordinate system of the images. The ROC plots show area under ROC curve versus threshold value for standard deviation or relative signal intensity.

Please cite this article in press as: Lund KV et al. Short-term pretreatment DCE-MRI in prediction of outcome in locally advanced cervical cancer. Radiother Oncol (2015), http://dx.doi.org/10.1016/j.radonc.2015.05.001

standard deviation in the EF-method (Fig. 1c) and 1.4 for relative signal intensity in the SI-method (Fig. 1d) when the analysis was based on LETV. When the analysis was based on LETF, the values were 3.5 for standard deviation in the EF-method (Supplementary Fig. 2c) and 1.3 for relative signal intensity in the SI-method (Supplementary Fig. 2d).

The LETVs determined by the EF-method and the SI-method were almost identical as were the LETFs. This is illustrated qualitatively and quantitatively in Fig. 2, which refers to LETVs and LETFs calculated by using the threshold values for standard deviation and relative signal intensity derived from the ROC analyses. The binary images in this figure refer to the high-enhancing (Fig. 2a) and low-enhancing (Fig. 2b) tumors depicted in Supplementary Fig. 1, and they show the low-enhancing voxels in black as determined by the EF-method (upper panels) and the SI-method (lower panels). There was a strong correlation between the LETVs ($P < 0.0001$, $R^2 = 0.92$, Fig. 2c) and between the LETFs ($P < 0.0001$, $R^2 = 0.93$, Fig. 2d) determined by these two methods for the 85 tumors included in our investigation.

Fig. 3 shows Kaplan–Meier curves for DFS and OS based on LETV calculated by using the threshold values determined by the ROC analysis. On the basis of the *P*-value images, the patient cohort was divided into a low tumor signal enhancement group (large LETVs) consisting of one third of the patients and a high tumor signal enhancement group (small LETVs) consisting of two thirds of the patients. The patients with small LETVs and those with large LETVs showed 5-year DFSs of 74% and 38%, respectively, and 5-year OSs of 79% and 39%, respectively, both when the LETVs were calculated by the EF-method (DFS: $P = 0.0009$, Fig. 3a; OS: $P < 0.0001$, Fig. 3b) and the SI-method (DFS: $P = 0.0013$, Fig. 3c; OS: $P = 0.0001$, Fig. 3d).

Equivalent Kaplan–Meier curves based on LETF are presented in Supplementary Fig. 3. The patients with small LETFs and those with large LETFs showed 5-year DFSs of 73% and 41%, respectively ($P = 0.0042$, Supplementary Fig. 3a), and 5-year OSs of 77% and 43%, respectively ($P = 0.0003$, Supplementary Fig. 3b), when the LETFs were calculated by the EF-method. The 5-year DFSs were 75% and 37%, respectively ($P = 0.0008$, Supplementary Fig. 3c), and the 5-year OSs were 79% and 39%, respectively ($P < 0.0001$, Supplementary Fig. 3d), when the LETFs were calculated by the SI-method.

Dichotomy around median LETV or median LETF provided poor association between clinical outcome and LETV or LETF compared with that observed by dividing the patient cohort into two groups consisting of one third and two thirds of the patients. The difference can be seen clearly from the *P*-value images. The *P*-values for DFS and OS pertaining to the two ways of dividing the patient cohort into a low and a high tumor signal enhancement group, calculated by using the threshold values for standard deviation and relative signal intensity derived from the ROC analyses, are compared in Supplementary Table 2.

Univariate Cox regression analysis of clinical parameters revealed that treatment outcome was influenced significantly by tumor volume, lymph node status, and FIGO stage, but not by tumor histology and patient age (Supplementary Table 3). Multivariate Cox regression analyses involving tumor volume, lymph node status, FIGO stage, and LETV (EF-method), LETF (EF-method), LETV (SI-method), or LETF (SI-method) were carried out to identify independent prognostic factors for DFS and OS (Table 1). The analyses showed that FIGO stage was the only clinical parameter that provided independent prognostic information on treatment outcome. Moreover, LETV (EF-method) and LETF (EF-method) were found to be independent prognostic factors for DFS, whereas the independent prognostic power of LETV (SI-method) and LETF (SI-method) for DFS were of borderline significance. The four DCE-MRI parameters were all strong independent prognostic factors for OS.

Discussion

Novel biomarkers for the outcome of chemoradiotherapy of locally advanced cervical cancer are needed for personalized treatment. DCE-MRI is a promising strategy, although conflicting observations have been reported [25–28]. Two semiquantitative methods of analysis of DCE-MRI data that have provided opposite conclusions were compared in this investigation: the EF-method of Donaldson et al. [26] and the SI-method of Mayr et al. [27]. Our study showed that these methods provide similar LETVs and LETFs. Moreover, we found that poor DFS and OS were associated with low tumor signal enhancement and that the prognostic power of LETV and LETF was independent of conventional prognostic factors such as tumor volume, lymph node status, and FIGO stage. Our observations were thus in good agreement with those of Mayr et al. [27], but contradictory to those of Donaldson et al. [26].

Assessment of the LETV and LETF of small tumors may involve significant uncertainties. Three of the 85 patients included in our study had tumors with volumes <5 cm^3 (1.5, 2.1, and 4.8 cm^3). The LETVs and LETFs of all 85 tumors were included when the *P*-values reported here were calculated. These *P*-values and our conclusions were not influenced significantly by the small tumors because *P*-values similar to those reported here were found when analyzing the data without including the three patients with small tumors.

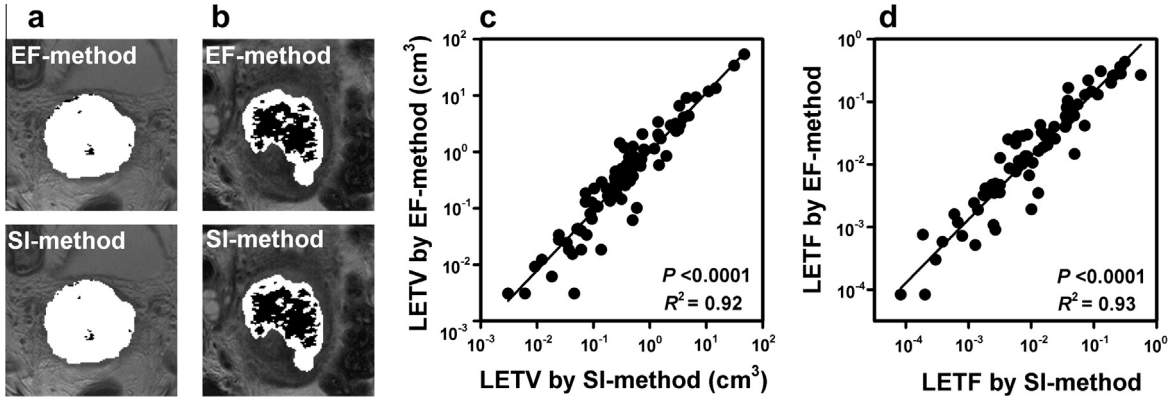

Fig. 2. Binary images of the high-enhancing (a) and low-enhancing (b) tumors depicted in Supplementary Fig. 1 showing the low-enhancing voxels in black as determined by the EF-method (upper panels) and the SI-method (lower panels). LETV determined by the EF-method versus LETV determined by the SI-method (c) and LETF determined by the EF-method versus LETF determined by the SI-method (d) for the 85 patients included in the investigation.

Please cite this article in press as: Lund KV et al. Short-term pretreatment DCE-MRI in prediction of outcome in locally advanced cervical cancer. Radiother Oncol (2015), http://dx.doi.org/10.1016/j.radonc.2015.05.001

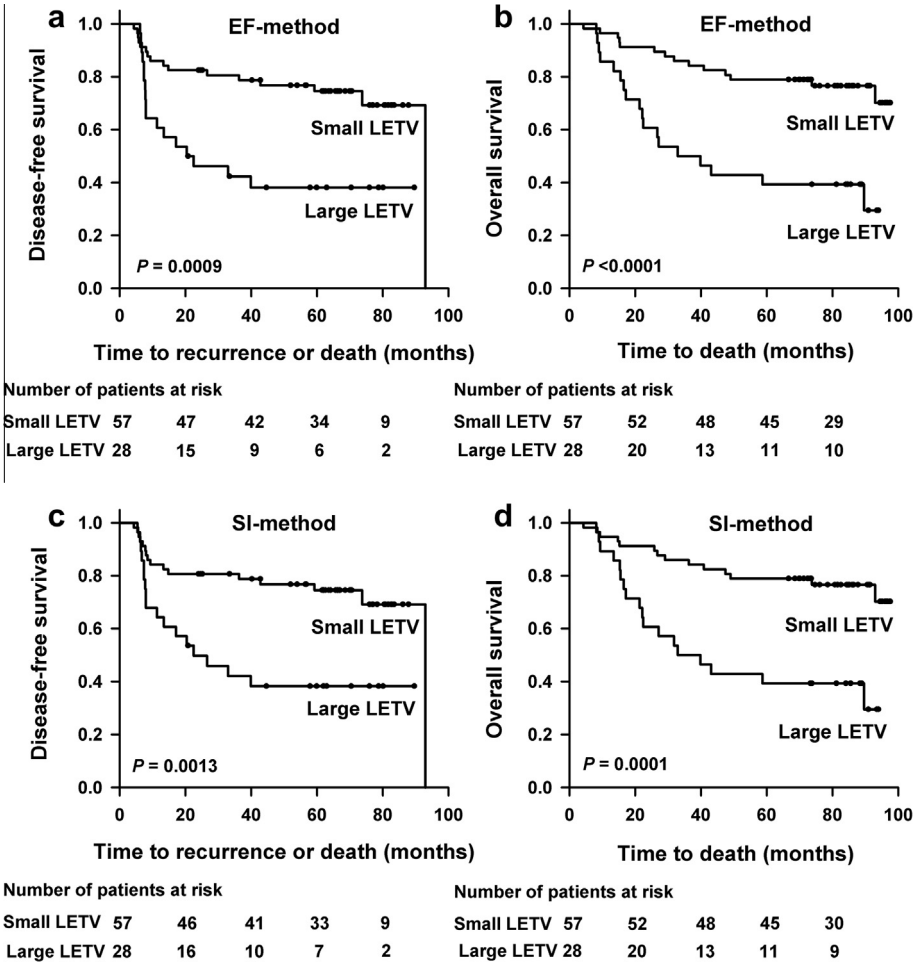

Fig. 3. Kaplan–Meier curves for DFS and OS stratified by LETV as calculated by the EF-method (a and b) and the SI-method (c and d). Small LETV, LETV < 0.6 cm^3 (EF-method) and LETV < 0.5 cm^3 (SI-method) ($N = 57$); large LETV, LETV > 0.7 cm^3 (EF-method) and LETV > 0.5 cm^3 (SI-method) ($N = 28$).

Table 1
Multivariate Cox regression analysis of clinical and DCE-MRI parameters.

	Disease-free survival				Overall survival			
	P-values				*P*-values			
Tumor volume	0.62	0.79	0.73	0.69	0.83	0.19	0.97	0.20
Lymph node status	0.38	0.52	0.40	0.37	0.93	0.66	0.99	0.92
FIGO stage	0.035	0.041	0.036	0.041	0.044	0.032	0.043	0.047
LETV (EF-method)	0.028				0.0012			
LETF (EF-method)		0.0029				<0.0001		
LETV (SI-method)			0.052				0.0022	
LETF (SI-method)				0.081				0.0013

Semiquantitative analysis of DCE-MRI recordings provides numerical values of parameters that are influenced by several factors, including the dose, relaxivity, and administration rate of the contrast agent, the strength of the magnetic field, and the MR sequence being used, and consequently, threshold values for tumor signal enhancement cannot be transferred between imaging centers without correction. The threshold value for EF used in our study differs from that used by Donaldson et al. [26]. It is unlikely that this difference can explain the contradictory conclusions, because our results were valid for a wide range of threshold values, as revealed by the *P*-value images. Moreover, the EF-values of Donaldson et al. [26] refer to the first post-contrast image, whereas we used the mean signal intensities of the first and second post-contrast images when calculating the data reported here. This difference can probably not explain the contradictory conclusions either, because our results are qualitatively similar independent of whether we calculate EF from the first, second, third, or fourth post-contrast image.

One should also be aware of other differences between this study and the study of Donaldson et al. [26]. The patients of Donaldson et al. [26] were treated with radiation therapy alone, whereas the patients included in our study were treated with concurrent chemoradiotherapy as were the patients of Mayr et al. [27]. Furthermore, our patient cohort was divided into two groups consisting of one third and two thirds of the patients, whereas the cohort studied by Donaldson et al. [26] was divided into two groups with one half of the patients in each group. The *P*-value images and Supplementary Table 2 suggest that dividing a cervical

Please cite this article in press as: Lund KV et al. Short-term pretreatment DCE-MRI in prediction of outcome in locally advanced cervical cancer. Radiother Oncol (2015), http://dx.doi.org/10.1016/j.radonc.2015.05.001

cancer patient cohort into two equally sized groups may be suboptimal for detecting associations between DCE-MRI-derived parameters and clinical outcome. It should also be noticed that the grouping used in our study is in accordance with the overall observation that standard first-line treatment fails in approximately one third of the patients with locally advanced cervical cancer [31].

In some studies, pharmacokinetic models have been used to analyze DCE-MRI series of locally advanced cervical carcinoma [21,23,24,28,32], and although many of these studies involved few patients, they suggest that poor response to treatment and/or survival is associated with low signal enhancement as did the study reported here. The main advantage of pharmacokinetic analysis is that the derived parametric images reflect characteristic properties of the tumor microenvironment such as blood perfusion, vascular permeability, and the fractional volume of the extravascular-extracellular space [19,33]. However, multiple different software packages with variation in mathematical modeling exist, and different models may produce dissimilar results [34]. Image acquisition at high temporal resolution for several minutes is needed for adequate pharmacokinetic analysis, and attractive models such as the Tofts model require assessment of a pre-contrast T_1-map and an arterial input function [35]. Furthermore, pharmacokinetic models are based on assumptions that are not necessarily fulfilled in tumor tissue [36]. For example, pharmacokinetic models may break down in tumor regions with necrotic tissue, and methods to eliminate such regions are needed to achieve valid parametric images of the tumor microenvironment [37].

In contrast to pharmacokinetic analyses, semiquantitative analyses of DCE-MRI series are easy to implement and may be used routinely at most imaging centers to provide biomarkers for the outcome of cancer treatment. An attractive feature of the analysis used in this study is that an acquisition period of only 1 min after the administration of contrast is sufficient to discriminate between patients with good and poor prognosis. CE-MRI is an established and commonly used method for anatomical characterization of the tumor tissue in cervical cancer patients, and by modest adaptations, functional characterization of the tumors can be accomplished routinely by introducing simple procedures for semiquantitative analysis of signal intensities. The main disadvantage of the procedure used in the present study, however, is that signal intensities are sensitive to the MR scanner and the MR protocol being used, implying that different hospitals have to establish and use their own individual signal intensity threshold values.

Measurements of tumor oxygen tension with Eppendorf electrodes have revealed that poor disease-free and overall survival rates in locally advanced cervical carcinoma are associated with extensive tumor hypoxia [5–10]. The present observation that low tumor signal enhancement is associated with treatment failure in cervical cancer patients is in full agreement with these studies. Tumor hypoxia is a result of an imbalance between the rate of oxygen supply and the rate of oxygen consumption [38]. Low tumor signal enhancement is a result of poor blood perfusion and/or a low extravascular-extracellular space fractional volume [35,36]. Poor perfusion indicates poor oxygen supply, and a small extravascular-extracellular space indicates high cell density and, consequently, high rates of oxygen consumption [37,38].

Moreover, preclinical studies have revealed that low tumor signal enhancement is associated with extensive hypoxia, poor radioresponsiveness, and elevated metastatic propensity in human cervical carcinoma xenografts [13,15,39]. In these studies, the fraction of hypoxic tumor cells was measured by the paired survival curve method [39] or by an immunohistochemical assay using pimonidazole as a hypoxia marker [13,15].

In future clinical studies, DCE-MRI should be combined with immunohistochemical analyses of the imaged tissue to investigate whether low tumor signal enhancement is associated with low microvascular density and extensive hypoxia also in human cervical carcinoma. If strong associations are found, LETV and LETF may be useful stratification parameters in studies investigating the potential benefits of using hypoxia-targeting treatment strategies together with chemoradiotherapy. Examples of such treatment strategies include the use of hypoxic cell sensitizers or other chemical hypoxic modifiers and the use of image-guided brachytherapy for dose escalation in hypoxic tumor regions.

Our study has several limitations. First, tumor ROIs were delineated on the basis of the signal intensity in T_2-weighted images. Although tumor tissue in general can be readily distinguished from the normal cervix parenchyma and adjacent air in T_2-weighted images, it is possible that low-signal-intensity regions in the tumor periphery were missed. Second, the DCE-MRI was carried out at a low temporal resolution of 29 s. Although our observations are independent of whether the analysis was based on the first, second, third, and/or the fourth post-contrast image, the peak signal intensity may have been missed. Third, only 85 patients were included in the study, and consequently, it needs validation in an independent cohort of patients. Despite these limitations, our investigation is an important proof-of-principle study highlighting low tumor signal enhancement as a strong prognostic factor for poor DFS and OS in cervical carcinoma patients treated with concurrent chemoradiotherapy.

In summary, the study reported in this communication shows that analysis of DCE-MRI data by the EF-method of Donaldson et al. [26] and the SI-method method of Mayr et al. [27] provides similar LETVs and similar LETFs in locally advanced cervical cancer and that poor DFS and OS are associated with large LETV and large LETF. Moreover, our investigation demonstrates that LETV and LETF determined from MR images acquired within 1 min after the administration of contrast have a strong prognostic effect for DFS and OS, independent of well-established prognostic factors such as tumor volume, lymph node status, and FIGO stage. Consequently, it is possible that biomarkers for personalized radiation therapy of cervical carcinoma can be derived by short-term pretreatment DCE-MRI without demanding image analysis or the use of advanced pharmacokinetic models.

Conflicts of interest statement

The authors have no conflicts of interest.

Acknowledgment

Financial support was received from the Norwegian Cancer Society and the South-Eastern Norway Regional Health Authority.

Appendix A. Supplementary data

Supplementary data associated with this article can be found, in the online version, at http://dx.doi.org/10.1016/j.radonc.2015.05.001.

References

[1] Eifel PJ. Concurrent chemotherapy and radiation therapy as the standard of care for cervical cancer. Nat Clin Pract Oncol 2006;3:248–55.
[2] Klopp AH, Eifel PJ. Biological predictors of cervical cancer response to radiation therapy. Semin Radiat Oncol 2012;22:143–50.
[3] Barwick TD, Taylor A, Rockall A. Functional imaging to predict tumor response in locally advanced cervical cancer. Curr Oncol Rep 2013;15:549–58.
[4] Vaupel P, Mayer A. Hypoxia in cancer: significance and impact on clinical outcome. Cancer Metastasis Rev 2007;26:225–39.
[5] Sundfør K, Lyng H, Rofstad EK. Tumour hypoxia and vascular density as predictors of metastasis in squamous cell carcinoma of the uterine cervix. Br J Cancer 1998;78:822–7.

[6] Pitson G, Fyles A, Milosevic M, Wylie J, Pintilie M, Hill R. Tumor size and oxygenation are independent predictors of nodal disease in patients with cervix cancer. Int J Radiat Oncol Biol Phys 2001;51:699–703.
[7] Höckel M, Knoop C, Schlenger K, et al. Intratumoral pO_2 predicts survival in advanced cancer of the uterine cervix. Radiother Oncol 1993;26:45–50.
[8] Fyles AW, Milosevic M, Wong R, et al. Oxygenation predicts radiation response and survival in patients with cervix cancer. Radiother Oncol 1998;48:149–56.
[9] Sundfør K, Lyng H, Tropé CG, Rofstad EK. Treatment outcome in advanced squamous cell carcinoma of the uterine cervix: relationships to pretreatment tumor oxygenation and vascularization. Radiother Oncol 2000;54:101–7.
[10] Nordsmark M, Loncaster J, Aquino-Parsons C, et al. The prognostic value of pimonidazole and tumour pO_2 in human cervix carcinomas after radiation therapy: a prospective international multi-center study. Radiother Oncol 2006;80:123–31.
[11] Ellingsen C, Egeland TAM, Galappathi K, Rofstad EK. Dynamic contrast-enhanced magnetic resonance imaging of human cervical carcinoma xenografts: pharmacokinetic analysis and correlation to tumor histomorphology. Radiother Oncol 2010;97:217–24.
[12] Hompland T, Ellingsen C, Øvrebø KM, Rofstad EK. Interstitial fluid pressure and associated lymph node metastasis revealed in tumors by dynamic contrast-enhanced MRI. Cancer Res 2012;72:4899–908.
[13] Ellingsen C, Walenta S, Hompland T, Mueller-Klieser W, Rofstad EK. The microenvironment of cervical carcinoma xenografts: associations with lymph node metastasis and its assessment by DCE-MRI. Trans Oncol 2013;6:607–17.
[14] Hompland T, Ellingsen C, Galappathi K, Rofstad EK. Connective tissue of cervical carcinoma xenografts: associations with tumor hypoxia and interstitial fluid pressure and its assessment by DCE-MRI and DW-MRI. Acta Oncol 2014;53:6–15.
[15] Ellingsen C, Hompland T, Galappathi K, Mathiesen B, Rofstad EK. DCE-MRI of the hypoxic fraction, radioresponsiveness, and metastatic propensity of cervical carcinoma xenografts. Radiother Oncol 2014;110:335–41.
[16] Hawighorst H, Knapstein PG, Weikel W, et al. Angiogenesis of uterine cervical carcinoma: characterization by pharmacokinetic magnetic resonance parameters and histological microvessel density with correlation to lymphatic involvement. Cancer Res 1997;57:4777–86.
[17] Cooper RA, Carrington BM, Loncaster JA, et al. Tumour oxygenation levels correlate with dynamic contrast-enhanced magnetic resonance imaging parameters in carcinoma of the cervix. Radiother Oncol 2000;57:53–5.
[18] Lyng H, Vorren AO, Sundfør K, et al. Assessment of tumor oxygenation in human cervical carcinoma by use of dynamic Gd-DTPA-enhanced MR imaging. J Magn Reson Imaging 2001;14:750–6.
[19] Zahra MA, Hollingsworth KG, Sala E, Lomas DJ, Tan LT. Dynamic contrast-enhanced MRI as a predictor of tumour response to radiotherapy. Lancet Oncol 2007;8:63–74.
[20] Yuh WTC, Mayr NA, Jarjoura D, et al. Predicting control of primary tumor and survival by DCE MRI during early therapy in cervical cancer. Invest Radiol 2009;44:343–50.
[21] Yamashita Y, Baba T, Baba Y, et al. Dynamic contrast-enhanced MR imaging of uterine cervical cancer: pharmacokinetic analysis with histopathologic correlation and its importance in predicting the outcome of radiation therapy. Radiology 2000;216:803–9.
[22] Mannelli L, Patterson AJ, Zahra M, et al. Evaluation of nonenhancing tumor fraction assessed by dynamic contrast-enhanced MRI subtraction as a predictor of decrease in tumor volume in response to chemoradiotherapy in advanced cervical cancer. AJR Am J Roentgenol 2010;195:524–7.
[23] Semple SIK, Harry VN, Parkin DE, Gilbert FJ. A combined pharmacokinetic and radiologic assessment of dynamic contrast-enhanced magnetic resonance imaging predicts response to chemoradiation in locally advanced cervical cancer. Int J Radiat Oncol Biol Phys 2009;75:611–7.
[24] Andersen EKF, Hole KH, Lund KV, et al. Pharmacokinetic parameters derived from dynamic contrast enhanced MRI of cervical cancers predict chemoradiotherapy outcome. Radiother Oncol 2013;107:117–22.
[25] Hawighorst H, Weikel W, Knapstein PG, et al. Angiogenic activity of cervical carcinoma: assessment by functional magnetic resonance imaging-based parameters and a histomorphological approach in correlation with disease outcome. Clin Cancer Res 1998;4:2305–12.
[26] Donaldson SB, Buckley DL, O'Connor JP, et al. Enhancing fraction measured using dynamic contrast-enhanced MRI predicts disease-free survival in patients with carcinoma of the cervix. Br J Cancer 2010;102:23–6.
[27] Mayr NA, Huang Z, Wang JZ, et al. Characterizing tumor heterogeneity with functional imaging and quantifying high-risk tumor volume for early prediction of treatment outcome: cervical cancer as a model. Int J Radiat Oncol Biol Phys 2012;83:972–9.
[28] Zahra MA, Tan LT, Priest AN, et al. Semiquantitative and quantitative dynamic contrast-enhanced magnetic resonance imaging measurements predict radiation response in cervix cancer. Int J Radiat Oncol Biol Phys 2009;74:766–73.
[29] Hompland T, Lund KV, Ellingsen C, Kristensen GB, Rofstad EK. Peritumoral interstitial fluid flow velocity predicts survival in cervical cancer. Radiother Oncol 2014;113:132–8.
[30] Rosset A, Spadola L, Ratib O. Osirix: an open-source software for navigating in multi dimensional DICOM images. J Digit Imaging 2004;17:205–16.
[31] Green JA, Kirwan JM, Tierney JF, et al. Survival and recurrence after concomitant chemotherapy and radiotherapy for cancer of the uterine cervix: a systematic review and meta-analysis. Lancet 2001;358:781–6.
[32] Loncaster JA, Carrington BM, Sykes JR, et al. Prediction of radiotherapy outcome using dynamic contrast enhanced MRI of carcinoma of the cervix. Int J Radiat Oncol Biol Phys 2002;54:759–67.
[33] Hylton N. Dynamic contrast-enhanced magnetic resonance imaging as an imaging biomarker. J Clin Oncol 2006;24:3293–8.
[34] Roberts C, Liyanage SH, Harry VN, Rockall AG. Functional imaging for assessing tumor response in cancer of the cervix. Women's Health 2011;7:487–97.
[35] Tofts PS, Brix G, Buckley DL, et al. Estimating kinetic parameters from dynamic contrast-enhanced T_1-weighted MRI of a diffusible tracer: standardized quantities and symbols. J Magn Reson Imaging 1999;10:223–32.
[36] Jennings D, Raghunand N, Gillies RJ. Imaging hemodynamics. Cancer Metastasis Rev 2008;27:589–613.
[37] Egeland TAM, Gulliksrud K, Gaustad JV, Mathiesen B, Rofstad EK. Dynamic contrast-enhanced-MRI of tumor hypoxia. Magn Reson Med 2012;67:519–30.
[38] Gulledge CJ, Dewhirst MW. Tumor oxygenation: a matter of supply and demand. Anticancer Res 1996;16:741–50.
[39] Ellingsen C, Egeland TAM, Gulliksrud K, Gaustad JV, Mathiesen B, Rofstad EK. Assessment of hypoxia in human cervical carcinoma xenografts by dynamic contrast-enhanced magnetic resonance imaging. Int J Radiat Oncol Biol Phys 2009;73:838–45.

Please cite this article in press as: Lund KV et al. Short-term pretreatment DCE-MRI in prediction of outcome in locally advanced cervical cancer. Radiother Oncol (2015), http://dx.doi.org/10.1016/j.radonc.2015.05.001